RESEARCH LETTER

Key Points:

- Land-surface temperature (LST) from ERA-5 Land are on average warmer than GOES-16 and 17 estimates, but for extremely hot conditions, ERA-5 underestimates LST
- ERA-5 Land does not accurately represent the magnitude and diurnal cycle of surface urban heat island effect
- GOES-16 and 17 show higher population exposure to extreme LST compared to ERA-5 Land

Supporting Information:

Supporting Information may be found in the online version of this article.

Correspondence to:

A. E. Dessler,
adessler@tamu.edu

Improved Surface Urban Heat Impact Assessment Using GOES Satellite Data: A Comparative Study With ERA-5

Jangho Lee[1] and Andrew E. Dessler[2]

[1]Department of Earth and Environmental Sciences, University of Illinois Chicago, Chicago, IL, USA, [2]Department of Atmospheric Sciences, Texas A&M University, College Station, TX, USA

Abstract We compare high-resolution land-surface temperature (LST) estimates from the GOES-16/17 (GOES) satellites to ERA-5 Land (ERA-5) reanalysis data across nine large US cities. We quantify the offset and find that ERA-5 generally overestimates LST compared to GOES by 1.63°C. However, this overestimation is less pronounced in urban areas, underscoring the limitations of ERA-5 in capturing the LST gradient between urban and non-urban areas. We then examine three quantities: Surface Urban Heat Island Intensity (SUHII), extreme LST events, and LST exposure by population. We find that ERA-5 does not accurately represent the diurnal variation and magnitude of SUHII in GOES. Furthermore, while ERA-5 was on average too warm, ERA-5 underestimates extreme heat by an average of 2.40°C. Our analysis reveals higher population exposure to high LST in the GOES data set across the cities studied. This discrepancy is especially pronounced when estimating the population fraction that are most exposed to heat.

1. Introduction

Reanalysis temperature data, such as the ERA-5 Land data (Muñoz-Sabater et al., 2021), have been widely used in studies of extreme heat (Ali et al., 2022; Lee & Dessler, 2023; Martinez & Iglesias, 2022; Raymond et al., 2020). Their primary advantage is the gridded format, lack of missing values, and the physical consistency provided by the underlying forecast model used in the data assimilation procedure.

However, reanalysis data have limitations, particularly when used in city-scale research, a crucial focal point considering over 80% of the US population lives in urban areas. The data assimilation process faces significant challenges in accurately representing urban climates due to the rural bias of weather stations and the sporadic coverage of polar-orbiting satellites (Hausfather et al., 2013). Additionally, inherent limitations of the underlying climate models (e.g., their resolution) can hinder the precise simulation of urban microclimates (Daniel et al., 2019). Thus, despite the apparent advantages of reanalysis data, their application in urban climate research and climate impact research presents notable obstacles.

Satellite observations, whether obtained by polar-orbiting or geostationary satellites, provide high-resolution estimates of surface temperature. The launch of the Geostationary Operational Environmental Satellite (GOES)-16 and 17 satellites (hereafter referred to collectively as GOES) significantly expanded the scope for detailed temperature observations across the US (Chang et al., 2021; Li et al., 2021; Yu et al., 2008; Zhang & Du, 2022). These satellites offer sub-hourly estimates, enabling nearly continuous monitoring of the surface. While the majority of earlier urban climate studies relied on data from polar-orbiting satellites like Moderate Resolution Imaging Spectroradiometer (MODIS) (Palou & Mahalov, 2019; Sidiqui et al., 2016; Tomlinson et al., 2012), or LandSat (Kaplan et al., 2018; Sagris & Sepp, 2017), the utilization of GOES remains relatively novel, with only a handful of studies capitalizing on its capabilities for similar research (Chang et al., 2021, 2022).

In our study, we compare GOES satellite estimates to ERA-5 reanalysis data across nine major cities in the United States and highlight the importance of high-resolution climate observations. Our investigation centers on four key questions: (a) estimating the general offset between the two data sets; (b) comparing the magnitude of the Surface Urban Heat Island Intensity (SUHII) in both data sets; (c) comparing the representation of extreme temperature events in both data sets; and (d) estimating the exposure to extreme temperature by population.

The reasons for focusing on these areas are manifold. First, a clear understanding of the general offset between the two data sets is of interest given the wide use of reanalysis. Second, given the significant contribution of SUHII to elevated city-level temperatures, it is imperative to assess how effectively reanalysis data sets capture

this phenomenon (Hsu et al., 2021; Li et al., 2017). Third, the accurate representation of extreme temperature events is crucial, as these events can have significant impacts on human health and city infrastructure (Lee & Dessler, 2023; Ma et al., 2015; Santágata et al., 2017; Sheridan & Allen, 2015; Stone Jr et al., 2021). Lastly, gauging the extent of population exposure to temperature extremes allows for an evaluation of public health risks and targeted interventions (Freychet et al., 2022; Jones et al., 2015; Tuholske et al., 2021).

1.1. Data

Our study utilizes hourly land surface temperature (LST) estimates from GOES-16 and -17 (Yu et al., 2008), which is provided on an irregular 2-km grid. Our analysis focuses on nine large US cities: Atlanta, Chicago, Dallas, Houston, Miami, Oklahoma City, Orlando, Phoenix, and Tampa. For these cities and their surrounding area, we extract LST data for the hot season (June, July, and August, or JJA) from 2018 to 2021. Total population of the nine cities is around 10M, which is about 3% of total US population. One inherent limitation of satellite estimates is the inability to capture surface data beneath cloud cover. Accordingly, we exclude cloudy pixels in our analysis using the GOES cloud mask. The average cloud-free LST during the study period for three of the nine cities is detailed in Figures 1a–1c.

We compare the GOES LST to LST fields from ERA-5 (Muñoz-Sabater et al., 2021). We use here the ERA-5 Land data set, a higher resolution derivative of the standard ERA-5 reanalysis (9 km for ERA-5 Land as opposed to 31 km for standard ERA-5). For simplicity, we will refer to the ERA-5 Land data set as simply "ERA-5" for the remaining sections of the paper. It's worth noting that the GOES-16 and GOES-17, which are employed in this study for comparison, are not assimilated into ERA-5, making GOES an independent data set. The ERA-5 data set is also provided on an hourly basis; however, its spatial resolution is $0.1° \times 0.1°$ latitude-longitude, coarser than that of GOES.

We will also use gridded population of the world version 4 (Doxsey-Whitfield et al., 2015) data from 2020. GPW is provided in 5-year intervals with 30 arc seconds resolution (approximately 1 km at the equator). To align the population grid to that of GOES grid, we take populations that are within a circle of $0.01°$ radius of each GOES grid points and sum the population to come up with population data at GOES resolution. The depiction of this population distribution can be observed in Figures 1g–1i.

Lastly, we incorporate land-cover data sourced from Sentinel-2 into our study (Karra et al., 2021). This data set comprises nine categories: water, trees, flooded vegetation, croplands, built areas, bare ground, snow/ice, and rangeland, all with a 10-m spatial resolution and provided every year. Given that these land cover data have a higher resolution than that of the GOES, we adjust its resolution to match GOES's. To do this, for the each GOES grid point, we take a circle around the grid point with a radius of $0.01°$. For the land cover within the circle, we compute the percentage distribution of the nine categories every year and select the most prevalent land cover type to represent that GOES grid point. The categories are visualized in Figures 1j–1l.

Although the land-cover data set includes nine land cover categories, our primary focus in this study is the "built area" category. Due to the high spatial resolution of the Sentinel-2 data, it identifies very small built areas nestled within non-urban zones. To filter these out, we employ a Gaussian kernel smoother to define the boundary of substantial built areas. Henceforth, we classify the grid points falling within this boundary as "Urban," and those outside this boundary as "non-Urban." The outcome of this urban, non-urban categorization is delineated by a black line in Figures 1j–1l. The plots for other cities in this study and number of GOES and ERA-5 pixels used in this analysis can be found in Supporting Information S1.

Since there is a difference between the spatial resolution of GOES and ERA-5, there are two ways to compare these data sets. First is to convert GOES to ERA-5 resolution, by averaging GOES grid points that surrounds each ERA-5 grid points. The second method is to convert ERA5 to GOES resolution by linearly interpolating the ERA-5 grid to the GOES grid. We found that there are no significant differences in the conclusions of this study when using the two methods, so, in places where it is required, we show results from converting GOES to ERA-5 resolution.

1.2. General LST Offset Between GOES and ERA-5

There is a clear offset in LST between GOES and ERA-5 (Figures 1a–1c vs. Figures 1d–1f). Figure 2 quantifies the difference between the two data sets, expressed as temporally averaged GOES LST minus temporally
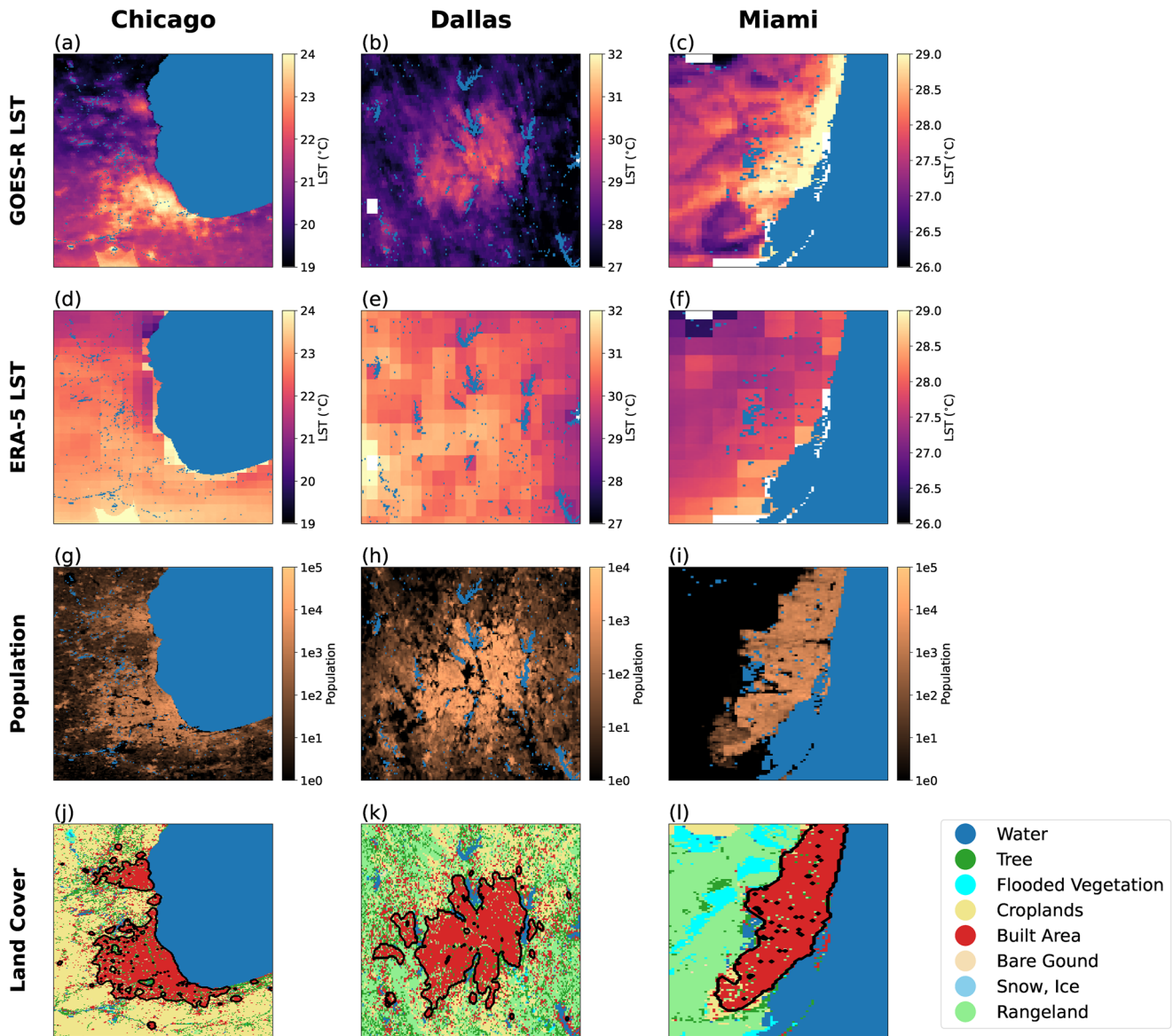
Figure 1. The average cloud-free land-surface temperature from GOES (a–c) and ERA-5 (d–f) during the study period. (g–i) Population counts with logarithmic color scales. (j–l) Land cover data, with the urban boundary, as defined by the Gaussian kernel, represented by a black line. Figures for the other cities can be found in Text S1 in Supporting Information S1.

averaged ERA-5 LST for the entire period. On average, ERA-5 is 1.63°C higher than GOES averaged across all urban regions in this study. City-specific values can be found below each figure.

While ERA-5 generally records a higher overall LST, the offset displays distinctive spatial characteristics. In urban areas, ERA-5 LST averages 1.16°C higher than GOES LST, while, in non-urban areas, this offset is 1.80°C. Given the demonstrated accuracy of GOES LST (Wang et al., 2019; Yu et al., 2011) and the widespread use of satellite-based LST in urban temperature analysis (Bechtel et al., 2019; Chang et al., 2021; Najafzadeh et al., 2021), it can be inferred that ERA-5 may have limitations in accurately capturing the LST gradient between urban and non-urban areas.

This discrepancy of LST offset (GOES minus ERA-5) between urban and non-urban area in Phoenix is not as evident compared to other cities (Figure 2h). This can be traced back to Phoenix's arid climate, as noted in previous study (Wang & Li, 2021).
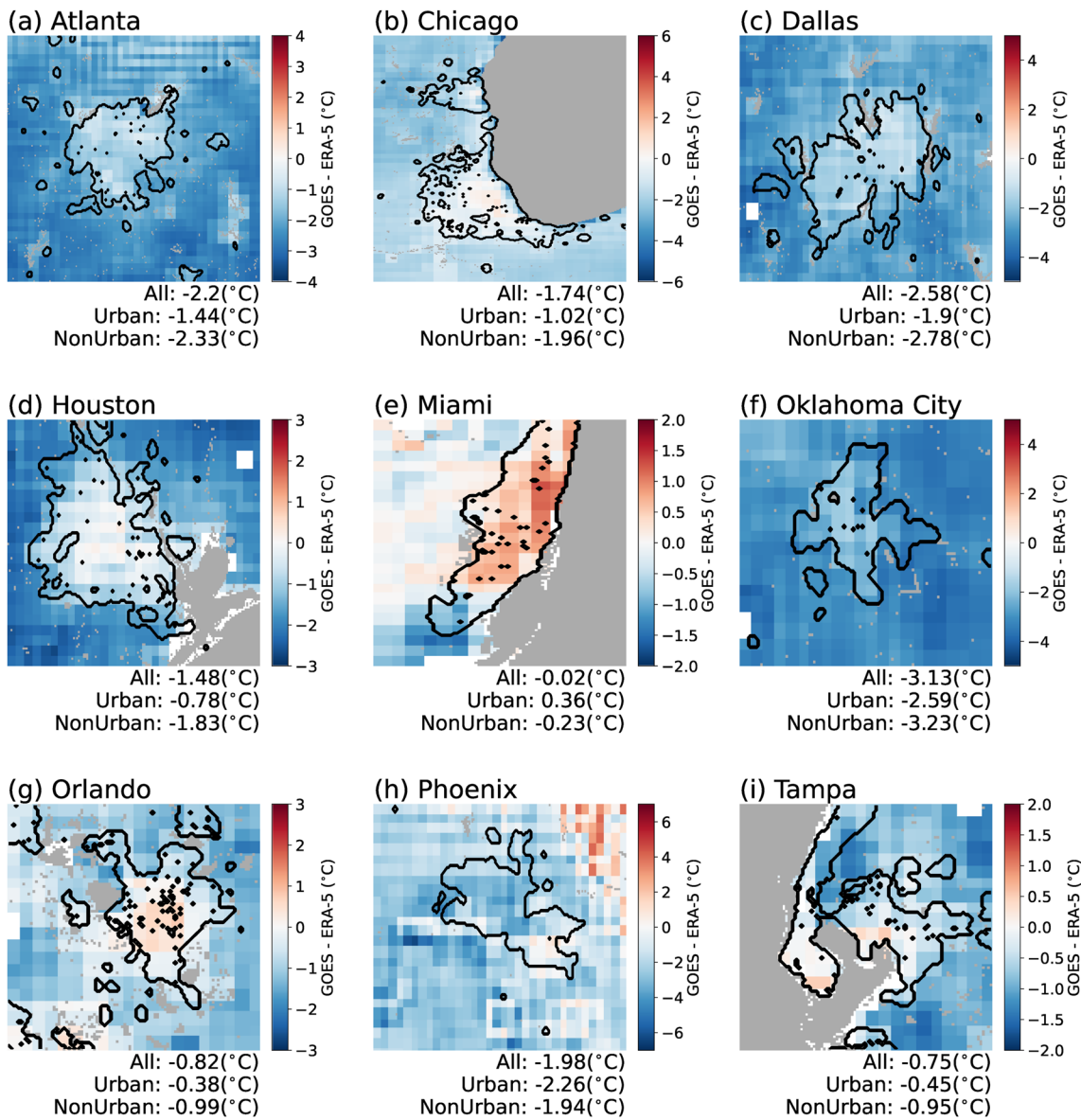
Figure 2. Spatial pattern of the average difference between cloud-free GOES and ERA-5 land-surface temperature (LST) throughout the study period, computed as GOES minus ERA-5. For this plot, GOES has been averaged to ERA5 resolution. Urban boundaries are demarcated by black lines and water bodies are masked out with a gray area. Offset of LST between GOES and ERA-5 are noted below each panel, where "All" representing the offset calculated from the entire region, "Urban" representing the offset within urban boundaries (black boundaries), and "NonUrban" representing the offset outside of urban boundaries. In all cases, water bodies are masked out from calculation.

1.3. Surface Urban Heat Island Effect

A key metric in urban climate impact studies is the SUHII, the difference between LST in an urban region and that in the surrounding non-urban area. To estimate the SUHII, we divide each city region into "urban" and "non-urban" areas (as defined in Figures 1j–1l). We then calculate the average LST for those areas on an hourly basis, determining the SUHII by subtracting the average non-urban LST from the urban LST, using data at ERA-5 resolution.

In our approach, when a boundary pixel contains a mix of urban and non-urban areas, we assign weights to the pixel's LST value for averaging purposes based on its land composition. For instance, if a boundary pixel is comprised of 70% urban and 30% non-urban areas, we calculate the urban average by multiplying the pixel's LST by 0.7, and the non-urban average by multiplying the same LST by 0.3. The height above sea level (elevation) can
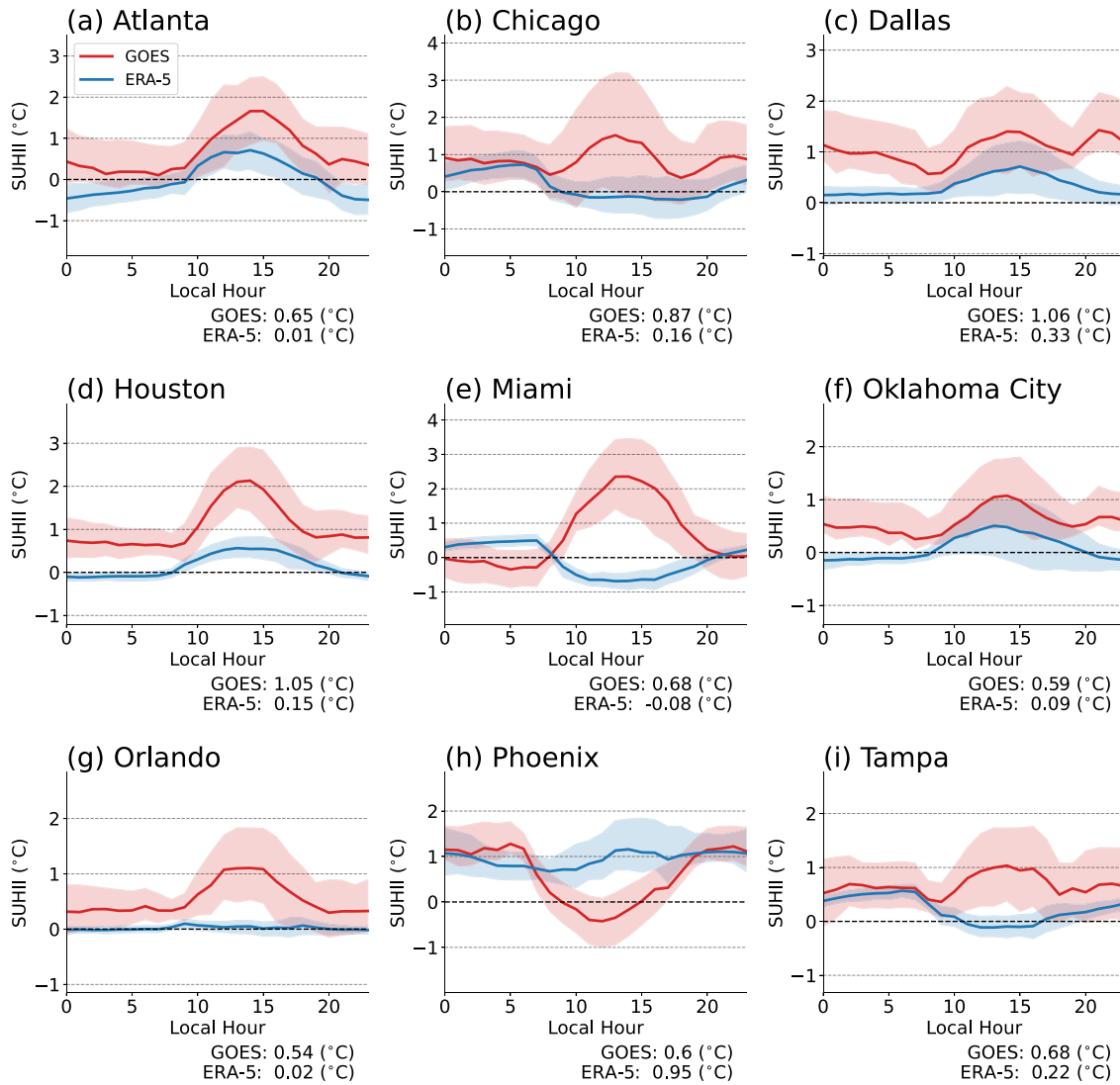
Figure 3. Diurnal cycle of UHII in ERA-5 (blue lines) and GOES (red lines) in nine cities. Solid lines show the average diurnal cycle calculated from the entire study period, and the shaded regions represent the first to third quantile range of hourly surface urban heat island intensity (SUHII) recorded in the study period. Average SUHII for GOES and ERA-5 are also shown below each figure.

impact SUHII, so we have also calculated impact of elevation on urban and non-urban LST. We found that including elevation does not significantly alter the outcomes of our study (see Text S2 in Supporting Information S1).

Figure 3 presents the diurnal cycle of the SUHII as represented by both GOES and ERA-5 LST data sets. As anticipated from Figures 1 and 2, GOES exhibits a higher SUHII than ERA-5, with a daily average SUHII for all cities of 0.74°C in GOES compared to 0.20°C for ERA-5. Values for the mean SUHII for each city region can also be found in Figure 3.

The SUHII diurnal cycle estimated from the GOES shows a few distinct diurnal cycle patterns. The first pattern, observed in Atlanta, Houston, Miami, Orlando, and Tampa, is characterized by a single major peak during the day, followed by a gradual decrease through the night. The second pattern, observed in Chicago, Dallas, and Oklahoma City, is marked by a significant peak during daytime and a second peak in the evening. Lastly, Phoenix exhibits a unique pattern where a minimum is observed during daytime.

These findings align with the categorization proposed by Liu et al. (2022) and Lai et al. (2018), which classified SUHII diurnal cycles based on patterns identified in major cities globally. They noted that the first pattern is typical of regions with a warm climate, and the second pattern is observed in cities with high population density or high

nighttime anthropogenic heat release. The last pattern, for Phoenix, tends to be prevalent in arid climate regions (Chow et al., 2012; Wang & Li, 2021), where the non-urban areas typically exhibit sparse vegetation and are predominantly characterized by bare ground. These terrains heat up quickly with sunrise, inducing a negative SUHII in the daytime. Conversely, in nighttime, urban infrastructure releases the accumulated heat from the day, while the bare ground, having retained less daytime heat, contributes less. This dynamic leads to heightened SUHII values during the night.

In some cases, ERA-5 has the right shape but smaller magnitude (in Atlanta, Dallas, Houston, and Oklahoma City); in others, the shape is wrong (in Chicago, Miami, Orlando, Phoenix, and Tampa). These findings underscore the risks of using reanalysis data to examine SUHI.

1.4. Extreme Heat Events

Extreme temperatures are a key driver of the health impacts of climate change (Ebi et al., 2021). Consequently, we are interested in determining the effectiveness of the GOES and ERA-5 data sets in accurately representing such extreme temperature events. To do this, we first compute the area-averaged (including urban and non-urban) LST for each hour over the duration of the study period using GOES data. To ensure that the majority of regions are not cloud covered in our analysis, hours with over 10% cloud cover in the region are excluded from this calculation. We then pinpointed the timestamps of the top 0.1% highest LST values in the GOES data, giving us the ~16 hottest hours for each city. Following this, we calculated the average LST field for both the ERA-5 and GOES data sets for these timestamps and averaged the GOES data to ERA-5 resolution before differencing the data sets. This method provides a city-specific estimate of the LST recorded by GOES and ERA-5 during the most intense heat events.

Figure 4 presents the LST differences between GOES and ERA-5 during instances of extreme heat, determined by subtracting ERA-5 LST from the GOES LST. The area-averaged LST from GOES exceed those from ERA-5 by an average of 2.40°C. This is quite different from the overall bias (Figure 2), where we observed ERA-5 typically measuring 1.63°C higher than GOES. Therefore, while ERA-5 on average shows higher LST, the situation is reversed during extreme heat events.

Focusing just on urban areas (demarcated by the black lines in Figure 4), the LST discrepancy between GOES and ERA-5 data is more pronounced, with GOES being on average 4.14°C higher than ERA-5. When using highest 1% LST hours from GOES, rather than 0.1%, GOES is 2.42°C hotter. Consistent with Figure 2, GOES LST typically exhibits a larger urban to non-urban LST gradient compared to ERA-5. Furthermore, as discussed in the previous section and in Figure 3, the SUHII is most pronounced during the hottest time of the day, explaining at least part of the offset between the data sets during extreme heat events.

Distinct LST discrepancies between GOES and ERA-5 are observed across various regions, often linked to land cover differences. Factors influencing these variations in extreme LST representation, such as trees and cropland, are detailed in Text S3 in Supporting Information S1. Our findings underscore that land cover plays a pivotal role in shaping how both GOES and ERA-5 represent extreme LST. Given ERA-5's biases, relying on it for estimating extreme LST events will likely underestimate their true magnitude. This has implications for studies that have used it to estimate the impacts from extreme heat (Lee & Dessler, 2023).

1.5. Population Exposure to Extreme Heat

Population density varies within cities. To reflect that, we now calculate the LST extreme heat exposure as a function of population. Utilizing the GOES data set, we isolate the hottest hour for each day throughout the entire study period from 2018 to 2021, which is typically between 12:00 and 16:00. With 92 days each year, this yields a total of 368 hr. From here, we leverage the gridded population data set to calculate the LST that the hottest 1%, 5%, 10%, and 25% of the population experience. This calculation is performed separately for each city (Figure 5). In this section, we analyze GOES LST data at its native resolution and compare it to ERA-5 linearly interpolated to GOES resolution, to more accurately reflect the spatial scale of population variations across each city.

We see higher LSTs in the GOES data set than in the ERA-5 data set in all cities for the hottest population, except for Phoenix. This can be attributed to Phoenix's arid climate, as discussed earlier. These differences seem likely to be the result of GOES' superior horizontal resolution. With a coarser grid, ERA5 will not resolve the very hottest temperature in a city, while GOES does.
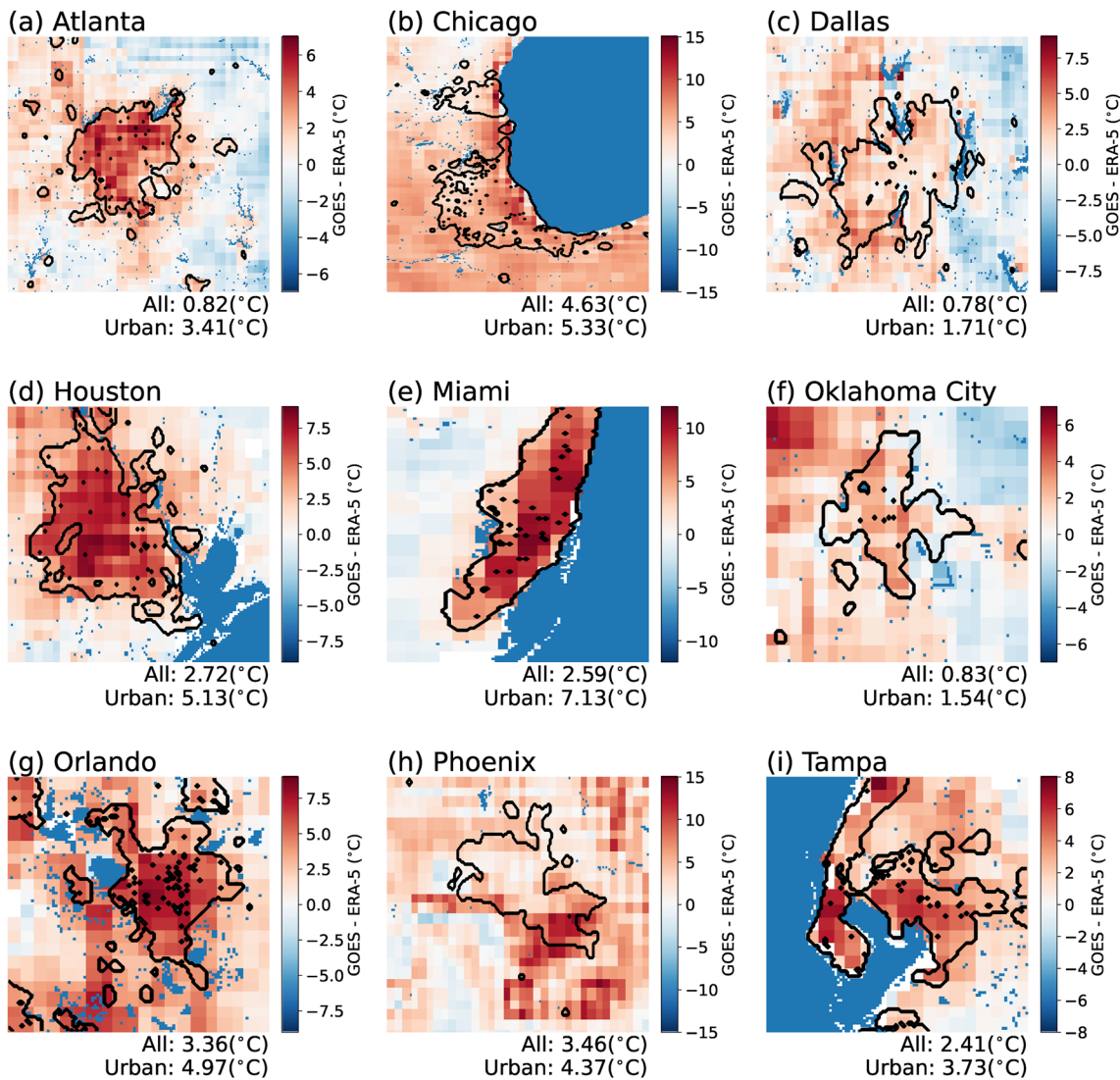
Figure 4. Land-surface temperature difference between GOES and ERA-5 data sets during extreme heat conditions, for each city, calculated as GOES minus ERA-5. The urban boundaries of each city are demarcated by a black line. Average difference between GOES and ERA-5 are noted below each panel, where "All" representing the offset calculated from the entire region, and "Urban" representing the offset within urban boundaries (black boundaries). For all cases, water bodies are masked out from calculation.

Considering larger fractions of the populations is equivalent to averaging over a larger area, so the discrepancy in LST exposure between the two data sets decreases. When looking at a large enough fraction of the population, the overall warm bias in ERA-5 LST reemerges, explaining why, for example, ERA-5 LST exceeds GOES for 25% of the population in Dallas and Oklahoma City.

In conclusion, choosing the GOES data set over ERA-5 produces hotter estimates for the hot end of the temperature distribution: an average of 3.58°C for the top 1% of the population and 2.91°C for the top 5% of the population (excluding Phoenix). This finding emphasizes the critical importance of high resolution when studying extreme heat exposure in urban populations.

In this section, we utilized both GOES and ERA-5 data sets at GOES resolution to reflect the detailed population distribution in urban areas. When re-gridding the GOES and population data sets to ERA-5 resolution, a similar yet less pronounced trend was observed.
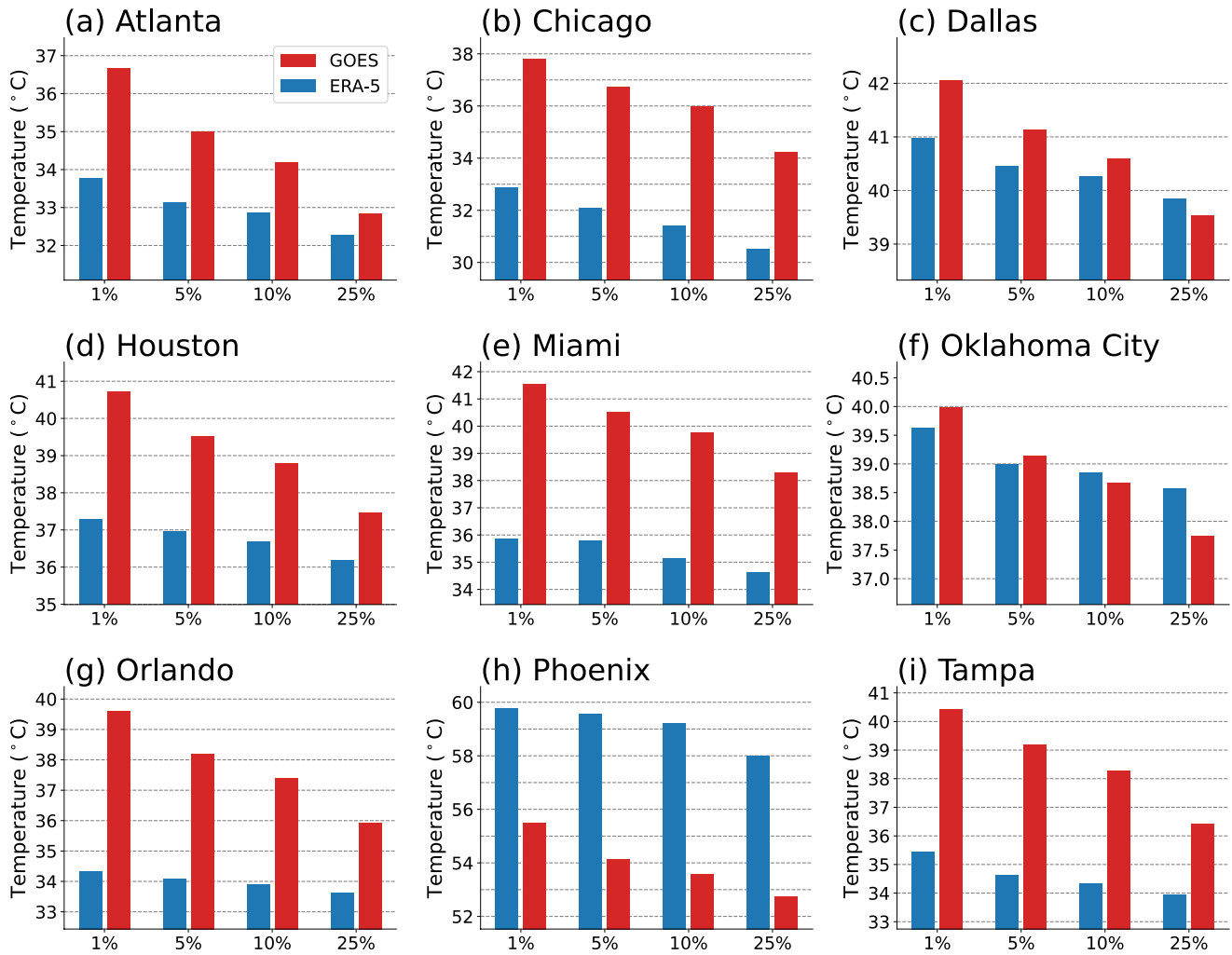
Figure 5. Average daily maximum land-surface temperature (LST) for the top 1%, 5%, 10%, and 25% of the population. The blue bars represent LST values obtained from the linearly interpolated ERA-5 data adapted to the GOES grid, while the red bars show LST values derived directly from the GOES data set.

2. Conclusion

In this study, we compared high-resolution satellite estimates of LST with estimates of this quantity from the ERA-5-land reanalysis. ERA-5 generally overestimates LST compared to GOES, with this difference less pronounced in urban areas. A consequence of this is that ERA-5 also underestimates the SUHII, the difference between the LST of an urban area and the non-urban surrounding region. We also find that ERA-5 does a poor job simulating the diurnal cycle of the SUHII.

Furthermore, while ERA-5 is generally hotter than GOES, we found that ERA-5 underestimates extreme hot conditions, a particularly important result since most of the damage of climate change comes from the extremes. Finally, our study's examination of urban population LST exposure showed consistently hotter temperatures in the GOES data compared to ERA-5 across all cities studied except Phoenix. The hottest 1% of the population experiences a 3.58°C higher LST during the hottest hour of the day, with this discrepancy diminishing when larger fractions of the population are considered. This pattern can likely be attributed to the finer resolution of GOES compared to ERA-5.

Our study reinforces the value of using high-resolution, high-accuracy data for urban climate impact assessments. This study also has its constraints. We analyzed LST around nine major US cities, each characterized by unique climatic conditions and urban layouts. Furthermore, the spatial resolution of GOES is 2 km, which might still not be sufficient for detailed neighborhood-level analysis. We also only consider LST, whereas 2-m air temperature

is expected to be more important in climate impact assessment. However, since GOES does not estimate 2-m air temperature, more work is needed in determining 2-m air temperature at high spatial resolution. We also only investigated temperature, not considering heat stress variables, such as wet-bulb temperature. Clearly, more research on this important topic of measuring surface urban heat is called for.

Conflict of Interest

The authors declare no conflicts of interest relevant to this study.

Data Availability Statement

GOES data used in this study are available to: GOES-R Algorithm Working Group & GOES-R Program office (2018). ERA-5 Land data are available to: Muñoz-Sabater (2019). Land cover data set is available to: Karra et al. (2021). Population data are available to: Gao and O'Neill (2020). Codes used in this analysis can be found in code repository: Lee and Dessler (2024).

References

Ali, M. A., Hassan, M., Mehmood, M., Kazmi, D. H., Chishtie, F. A., & Shahid, I. (2022). The potential impact of climate extremes on cotton and wheat crops in Southern Punjab, Pakistan. *Sustainability*, *14*(3), 1609. https://doi.org/10.3390/su14031609

Bechtel, B., Demuzere, M., Mills, G., Zhan, W., Sismanidis, P., Small, C., & Voogt, J. (2019). SUHI analysis using local climate zones—A comparison of 50 cities. *Urban Climate*, *28*, 100451. https://doi.org/10.1016/j.uclim.2019.01.005

Chang, Y., Xiao, J., Li, X., Frolking, S., Zhou, D., Schneider, A., et al. (2021). Exploring diurnal cycles of surface urban heat island intensity in Boston with land surface temperature data derived from GOES-R geostationary satellites. *Science of the Total Environment*, *763*, 144224. https://doi.org/10.1016/j.scitotenv.2020.144224

Chang, Y., Xiao, J., Li, X., Zhou, D., & Wu, Y. (2022). Combining GOES-R and ECOSTRESS land surface temperature data to investigate diurnal variations of surface urban heat island. *Science of the Total Environment*, *823*, 153652. https://doi.org/10.1016/j.scitotenv.2022.153652

Chow, W. T., Brennan, D., & Brazel, A. J. (2012). Urban heat island research in Phoenix, Arizona: Theoretical contributions and policy applications. *Bulletin of the American Meteorological Society*, *93*(4), 517–530. https://doi.org/10.1175/bams-d-11-00011.1

Daniel, M., Lemonsu, A., Déqué, M., Somot, S., Alias, A., & Masson, V. (2019). Benefits of explicit urban parameterization in regional climate modeling to study climate and city interactions. *Climate Dynamics*, *52*(5–6), 2745–2764. https://doi.org/10.1007/s00382-018-4289-x

Doxsey-Whitfield, E., MacManus, K., Adamo, S. B., Pistolesi, L., Squires, J., Borkovska, O., & Baptista, S. R. (2015). Taking advantage of the improved availability of census data: A first look at the gridded population of the world, version 4. *Papers in Applied Geography*, *1*(3), 226–234. https://doi.org/10.1080/23754931.2015.1014272

Ebi, K. L., Capon, A., Berry, P., Broderick, C., de Dear, R., Havenith, G., et al. (2021). Hot weather and heat extremes: Health risks. *The Lancet*, *398*(10301), 698–708. https://doi.org/10.1016/s0140-6736(21)01208-3

Freychet, N., Hegerl, G. C., Lord, N. S., Lo, Y. E., Mitchell, D., & Collins, M. (2022). Robust increase in population exposure to heat stress with increasing global warming. *Environmental Research Letters*, *17*(6), 064049. https://doi.org/10.1088/1748-9326/ac71b9

Gao, J., & O'Neill, B. C. (2020). Mapping global urban land for the 21st century with data-driven simulations and Shared Socioeconomic Pathways [Dataset]. Nature Communications. https://sedac.ciesin.columbia.edu/data/collection/gpw-v4

GOES-R Algorithm Working Group, & GOES-R Program Office. (2018). NOAA Geostationary Operational Environmental Satellite (GOES-16) series Advanced Baseline Imager (ABI) level 2 Land Surface Temperature (LST) [Dataset]. https://doi.org/10.7289/V52R3PZ8

Hausfather, Z., Menne, M. J., Williams, C. N., Masters, T., Broberg, R., & Jones, D. (2013). Quantifying the effect of urbanization on US Historical Climatology Network temperature records. *Journal of Geophysical Research: Atmospheres*, *118*(2), 481–494. https://doi.org/10.1029/2012jd018509

Hsu, A., Sheriff, G., Chakraborty, T., & Manya, D. (2021). Disproportionate exposure to urban heat island intensity across major US cities. *Nature Communications*, *12*(1), 2721. https://doi.org/10.1038/s41467-021-22799-5

Jones, B., O'Neill, B. C., McDaniel, L., McGinnis, S., Mearns, L. O., & Tebaldi, C. (2015). Future population exposure to US heat extremes. *Nature Climate Change*, *5*(7), 652–655. https://doi.org/10.1038/nclimate2631

Kaplan, G., Avdan, U., & Avdan, Z. Y. (2018). Urban heat island analysis using the Landsat 8 satellite data: A case study in Skopje, Macedonia. In *Proceedings* (Vol. 2, p. 358). MDPI.

Karra, K., Kontgis, C., Statman-Weil, Z., Mazzariello, J. C., Mathis, M., & Brumby, S. P. (2021). Global land use/land cover with Sentinel 2 and deep learning [Dataset]. IEEE. https://www.arcgis.com/home/item.html?id=cfcb7609de5f478eb7666240902d4d3d

Lai, J., Zhan, W., Huang, F., Voogt, J., Bechtel, B., Allen, M., et al. (2018). Identification of typical diurnal patterns for clear-sky climatology of surface urban heat islands. *Remote Sensing of Environment*, *217*, 203–220. https://doi.org/10.1016/j.rse.2018.08.021

Lee, J., & Dessler, A. E. (2023). Future temperature-related deaths in the US: The impact of climate change, demographics, and adaptation. *GeoHealth*, *7*(8), e2023GH000799. https://doi.org/10.1029/2023gh000799

Lee, J., & Dessler, A. (2024). Improved Surface Urban Heat Impact Assessment Using GOES Satellite Data: A Comparative Study With ERA-5. *Zenodo*. https://doi.org/10.5281/ZENODO.10463900

Li, K., Guan, K., Jiang, C., Wang, S., Peng, B., & Cai, Y. (2021). Evaluation of four new land surface temperature (LST) products in the US corn belt: ECOSTRESS, GOES-R, Landsat, and Sentinel-3. *IEEE Journal of Selected Topics in Applied Earth Observations and Remote Sensing*, *14*, 9931–9945. https://doi.org/10.1109/jstars.2021.3114613

Li, X., Zhou, Y., Asrar, G. R., Imhoff, M., & Li, X. (2017). The surface urban heat island response to urban expansion: A panel analysis for the conterminous United States. *Science of the Total Environment*, *605*, 426–435. https://doi.org/10.1016/j.scitotenv.2017.06.229

Liu, Z., Zhan, W., Lai, J., Bechtel, B., Lee, X., Hong, F., et al. (2022). Taxonomy of seasonal and diurnal clear-sky climatology of surface urban heat island dynamics across global cities. *ISPRS Journal of Photogrammetry and Remote Sensing*, *187*, 14–33. https://doi.org/10.1016/j.isprsjprs.2022.02.019

Ma, G., Rudolf, V. H., & Ma, C. S. (2015). Extreme temperature events alter demographic rates, relative fitness, and community structure. *Global Change Biology*, *21*(5), 1794–1808. https://doi.org/10.1111/gcb.12654

Martinez, A., & Iglesias, G. (2022). Climate change impacts on wind energy resources in North America based on the CMIP6 projections. *Science of the Total Environment*, *806*, 150580. https://doi.org/10.1016/j.scitotenv.2021.150580

Muñoz-Sabater, J. (2019). ERA5-Land hourly data from 1950 to present. Copernicus climate change service (C3S) climate data store (CDS) [Dataset]. https://doi.org/10.24381/cds.e2161bac

Muñoz-Sabater, J., Dutra, E., Agustí-Panareda, A., Albergel, C., Arduini, G., Balsamo, G., et al. (2021). ERA5-Land: A state-of-the-art global reanalysis dataset for land applications. *Earth System Science Data*, *13*(9), 4349–4383. https://doi.org/10.5194/essd-13-4349-2021

Najafzadeh, F., Mohammadzadeh, A., Ghorbanian, A., & Jamali, S. (2021). Spatial and temporal analysis of surface urban heat island and thermal comfort using Landsat satellite images between 1989 and 2019: A case study in Tehran. *Remote Sensing*, *13*(21), 4469. https://doi.org/10.3390/rs13214469

Palou, F. S., & Mahalov, A. (2019). Summer-and wintertime variations of the surface and near-surface urban heat island in a semiarid environment. *Weather and Forecasting*, *34*(6), 1849–1865. https://doi.org/10.1175/waf-d-19-0054.1

Raymond, C., Matthews, T., & Horton, R. M. (2020). The emergence of heat and humidity too severe for human tolerance. *Science Advances*, *6*(19), eaaw1838. https://doi.org/10.1126/sciadv.aaw1838

Sagris, V., & Sepp, M. (2017). Landsat-8 TIRS data for assessing Urban Heat Island effect and its impact on human health. *IEEE Geoscience and Remote Sensing Letters*, *14*(12), 2385–2389. https://doi.org/10.1109/lgrs.2017.2765703

Santágata, D. M., Castesana, P., Rössler, C. E., & Gómez, D. R. (2017). Extreme temperature events affecting the electricity distribution system of the metropolitan area of Buenos Aires (1971–2013). *Energy Policy*, *106*, 404–414. https://doi.org/10.1016/j.enpol.2017.04.006

Sheridan, S. C., & Allen, M. J. (2015). Changes in the frequency and intensity of extreme temperature events and human health concerns. *Current Climate Change Reports*, *1*(3), 155–162. https://doi.org/10.1007/s40641-015-0017-3

Sidiqui, P., Huete, A., & Devadas, R. (2016). Spatio-temporal mapping and monitoring of urban heat island patterns over Sydney, Australia using MODIS and Landsat-8. In *2016 4th International Workshop on Earth observation and Remote Sensing applications (EORSA)* (pp. 217–221). IEEE.

Stone, B., Jr., Mallen, E., Rajput, M., Gronlund, C. J., Broadbent, A. M., Krayenhoff, E. S., et al. (2021). Compound climate and infrastructure events: How electrical grid failure alters heat wave risk. *Environmental Science & Technology*, *55*(10), 6957–6964. https://doi.org/10.1021/acs.est.1c00024

Tomlinson, C., Chapman, L., Thornes, J., & Baker, C. (2012). Derivation of Birmingham's summer surface urban heat island from MODIS satellite images. *International Journal of Climatology*, *32*(2), 214–224. https://doi.org/10.1002/joc.2261

Tuholske, C., Caylor, K., Funk, C., Verdin, A., Sweeney, S., Grace, K., et al. (2021). Global urban population exposure to extreme heat. *Proceedings of the National Academy of Sciences*, *118*(41), e2024792118. https://doi.org/10.1073/pnas.2024792118

Wang, H., Yu, Y., Yu, P., & Liu, Y. (2019). Land surface emissivity product for NOAA JPSS and GOES-R missions: Methodology and evaluation. *IEEE Transactions on Geoscience and Remote Sensing*, *58*(1), 307–318. https://doi.org/10.1109/tgrs.2019.2936297

Wang, L., & Li, D. (2021). Urban heat islands during heat waves: A comparative study between Boston and Phoenix. *Journal of Applied Meteorology and Climatology*, *60*(5), 621–641. https://doi.org/10.1175/jamc-d-20-0132.1

Yu, Y., Tarpley, D., Privette, J. L., Flynn, L. E., Xu, H., Chen, M., et al. (2011). Validation of GOES-R satellite land surface temperature algorithm using SURFRAD ground measurements and statistical estimates of error properties. *IEEE Transactions on Geoscience and Remote Sensing*, *50*(3), 704–713. https://doi.org/10.1109/tgrs.2011.2162338

Yu, Y., Tarpley, D., Privette, J. L., Goldberg, M. D., Raja, M. R. V., Vinnikov, K. Y., & Xu, H. (2008). Developing algorithm for operational GOES-R land surface temperature product. *IEEE Transactions on Geoscience and Remote Sensing*, *47*(3), 936–951.

Zhang, Z., & Du, Q. (2022). Hourly mapping of surface air temperature by blending geostationary datasets from the two-satellite system of GOES-R series. *ISPRS Journal of Photogrammetry and Remote Sensing*, *183*, 111–128. https://doi.org/10.1016/j.isprsjprs.2021.10.022